

A Numerical Continuation Method to Compute Nonlinear Normal Modes Using Modal Reduction

Matthew S. Allen¹,
Robert J. Kuether²,
Brandon Deaner³,

Engineering Physics Department, University of Wisconsin-Madison, Madison, Wisconsin, 53706, USA
&

Michael W. Sracic⁴
Belcan Engineering Group, Inc., Indianapolis, IN, 46241, USA

Nonlinearities in structural dynamic systems introduce behavior that cannot be described with linear vibration theory, such as frequency-energy dependence and internal resonances. The concept of nonlinear normal modes accommodates such phenomena, providing a rigorous framework to characterize and design nonlinear structures. A recently developed method has enabled the computation of nonlinear normal modes for structures with hundreds of degrees of freedom, but the formulation is not readily applicable to large scale geometrically nonlinear structures that are modeled within finite element software. This work presents a variation on that approach that can be used to extract the nonlinear normal modes of a structure using commercial finite element software. A model of the structure is created in the finite element package and the algorithm then iterates on the nonlinear transient response in a non-intrusive way to estimate the nonlinear modes. A modal coordinate transformation is used to reduce the order of the Jacobians required by the algorithm. The method is demonstrated on a fixed-fixed beam that is geometrically nonlinear due to coupling between transverse and axial displacements. An alternative procedure is also presented in which static load cases are used to compute a reduced order model of the nonlinear system and then standard continuation is used to find the nonlinear modes of the reduced order model. That approach is explored using both enforced displacements and applied loads and the results obtained are compared with those from the full-order model.

I. Introduction

NONLINEARITIES are important in a wide range of structures. Some common sources of nonlinearities are large deformation effects, bolted joints, and nonlinear material constitutive laws. For example, the skin of high speed aircraft can buckle due to aerothermal heating leading to highly nonlinear behavior even when the material is within its elastic limit [1]. Similarly, friction and bolted/riveted joints in engineering structures can introduce nonlinear damping or stick-slip nonlinearity [2, 3]. Nonlinearities can dramatically alter the response of a system, causing it to exhibit behavior that cannot be described by linear vibration theory, such as bifurcations, internal resonances and frequency-energy dependence. These must be properly accounted for in order to accurately predict a structure's response.

This work is motivated by the need to improve the performance of the skin panels of future hypersonic vehicles. These skin panels are subjected to significant heating which can cause them to buckle and vibrate nonlinearly in response to pressure fluctuations in the flow field during flight [1, 4, 5], making their response and hence their life

¹Assistant Professor, 535 Engineering Research Building, 1500 Engineering Drive, Madison, WI 53706-1609, msallen@engr.wisc.edu, AIAA Member.

²Graduate Student, 534 ERB, rkuether@wisc.edu, AIAA Student Member.

³Graduate Student, 534 ERB, bdeaner@wisc.edu, AIAA Student Member.

⁴Analytical Design Engineer, 5420 W. Southern Avenue, Suite 400, Indianapolis, IN, 46241-5569, mwsracic@gmail.com.

difficult to predict. A buckled structure typically has multiple stable equilibrium positions and nonlinearities must be considered to predict the structure's response as it jumps between the equilibrium states. A careful design is required to assure that the structure can withstand the in-flight loads while not exceeding weight requirements.

Nonlinear Normal Modes provide a lot of insight into the behavior of a nonlinear structure. This work uses the undamped nonlinear normal mode concept originally defined by Rosenberg [6] and further developed by Vakakis, Kerschen and others [7, 8]. According to their definition, a nonlinear normal mode (NNM) is a not necessarily synchronous periodic response of the undamped nonlinear system. Once the NNMs of a system are known, one can predict much of the frequency content in the structure's free response. The NNMs are also related to the backbone curves of the structure's nonlinear frequency response, so they provide important insights into the structure's forced response. Vakakis et al. recently used the NNM concept to design a special class of nonlinear vibration absorbers called "nonlinear energy sinks" [9]. The NNM concept has also been extended to damped normal modes [10] and studied in conjunction with forced response [11] and model reduction [12].

Nonlinear normal modes have traditionally been found using analytical techniques, such as the method of multiple scales [7, 8, 13, 14] or the harmonic balance technique [15]. These analytical methods are typically only applicable to relatively simple structures, i.e. situations in which the equations of motion can be written in closed form. Recently, Peeters et al. developed an alternative based on numerical integration, shooting and a pseudo-arclength continuation technique [16], which has been shown to perform well for quite complicated structures. Their method was recently used to compute the first several NNMs of a reduced order model of an aircraft with 548 degrees of freedom [17]. They accomplished this by creating a detailed finite element model of the aircraft and then reducing it to a 548 degree of freedom Craig-Bampton [18] model. Discrete nonlinear springs were then added between the wings and fuel tanks.

This work extends the approach of Peeters et al. to systems with geometric nonlinearity that are modeled in commercial finite element codes. The Craig-Bampton approach employed in [17] cannot be used to obtain a nonlinear reduced order model for a system with global nonlinearities. The method presented in this work deals directly with the full order nonlinear finite element model in the native finite element code. The finite element code is used to numerically compute the response of the system to various initial conditions, and a shooting technique similar to that employed by Peeters et al. is used to find those initial conditions that produce a periodic response (or a nonlinear normal mode). Note that the equations of motion do not exist in closed form but within the finite element code; the finite element software integrates the equations of motion without constructing a mathematical model of the usual sort. Because of this, the algorithm employed by Peeters et al. to compute the Jacobian of the shooting function cannot be used, as it requires the derivative of the equations of motion. In order to have a non-intrusive approach, this work employs finite differences instead. This could be problematic if the state vector of the system was comprised of the displacements of each of the individual nodes of the system, since perturbing each node of a large finite element model would be very expensive. Also, perturbing only one node of a finite element model might excite very high frequency modes requiring a very small time step to obtain a valid solution. To circumvent this difficulty, this work uses a set of modal coordinates based on the linear modes of the structure. Each nonlinear normal mode originates at a linear mode at very low energy, so the algorithm initially uses only one coordinate for each NNM. As energy increases the algorithm monitors the numerically integrated time responses and augments the coordinate set as other modes begin to contribute significantly. Ideally, by reducing the number of degrees of freedom (DOF) one can achieve a dramatic reduction in the computational burden for systems with a large number of physical DOF. This would enable computation of NNMs for far more complicated structures. This new approach will be called the full-modal continuation method (FMCN).

One alternative to the algorithm proposed here is to compute a nonlinear reduced order model (ROM) for the structure from the solutions to a set of static load cases [19]. Then conventional methods could be used to find the nonlinear modes of the ROM. (While ROMs such as those described in [19] have been used in many studies to predict the response of a nonlinear structure, the authors are not aware of a work in which the ROMs have been used to compute nonlinear normal modes.) Two ROM methods were explored in this work and compared with the FMCN approach. The first method is by McEwan [20] and is referred to as the applied loads procedure in [19] or as Implicit Condensation (IC) in [1]. The second method is by Muravyov and Rizzi [21] and is referred to as the enforced displacements procedure in [19]. In both cases, nonlinear static solutions are used to solve for a set of nonlinear stiffness coefficients that capture the nonlinearity in the system.

The paper is organized as follows. Section II discusses the development of the FMCN algorithm, and the interface between the algorithm and a nonlinear FEA package. Section III briefly reviews the two reduced order modeling methods that are used in this work. The FMCN method is then evaluated using a nonlinear 11DOF lumped mass system with cubic nonlinearities and a geometrically nonlinear beam modeled in ANSYS. The results

and observations are presented in Section IV. In Section V, the NNMs of the beam are computed from the reduced order models and compared with the results of the FMCM algorithm. Conclusions are then presented in Section VI.

II. Numerical Computations of NNMs Using Modal Coordinates

This work is based on the numerical continuation approach presented by Peeters et al. [16], which is applicable to a broad class of autonomous, conservative nonlinear systems. These systems are described by the state space differential equation

$$\dot{z} = f(t, z_0) \quad (1)$$

where z is the time dependent state vector, z_0 is the initial conditions vector, $f()$ is a nonlinear function of the states and t is the time variable. An NNM is defined by the period T and initial conditions z_0 which produce a periodic response, $z_p(t+T, z_0) = z_p(t, z_0)$. For a structural dynamic system, the state vector $z = [x^T \ \dot{x}^T]^T$ is comprised of physical displacements x and velocities \dot{x} , where $()^T$ represents the transpose operation. A system with N -DOF will have $2N$ states, which will be described using a modal coordinate transformation. The linear mode shape matrix Φ ($N \times N$ matrix) is computed from the undamped, linearized equation of motion (i.e. for small displacements about an equilibrium position) from the linearized mass and stiffness matrices M and K . A coordinate transformation is then used to represent the physical displacements and velocities in terms of the *linear* modal coordinates.

$$x = \Phi q \quad (2)$$

$$\dot{x} = \Phi \dot{q} \quad (3)$$

Hence the $2N \times 1$ state vector is transformed to modal displacements q and modal velocities \dot{q} , and is generalized as $z = [\Phi q^T \ \Phi \dot{q}^T]^T$. It is often the case that far fewer modes contribute significantly to a response than there are physical degrees of freedom, so this coordinate change would be expected to reduce the order of the system dramatically. Since an NNM solution branch is initiated at a linear mode at low energy, the initial modal amplitudes for the n th NNM branch can be taken to be

$$(q_0)_r = \begin{cases} q_{n0} & n = r \\ 0 & n \neq r \end{cases} \quad (4)$$

where the initial modal amplitude of the n^{th} linear mode, q_{n0} , is small enough to assure that the system's response is well approximated as linear. Using a modal basis, the initial conditions can be written in terms of modal states as

$$z_0 = \begin{bmatrix} \Phi & 0 \\ 0 & \Phi \end{bmatrix} \begin{Bmatrix} q_0 \\ \dot{q}_0 \end{Bmatrix} \quad (5)$$

A periodic solution for a nonlinear system is implicitly dependent on the initial conditions, z_0 , and period of oscillation, T . In order to obtain a unique solution, the phase of the periodic solution is fixed by setting $\dot{q}_0 = 0$. This also improves the computational efficiency of the algorithm by further reducing the number of free parameters in Eq. (5). A periodic solution to the autonomous, conservative nonlinear equations of motion is sought such that

$$z_p(t+T, q_0) = z_p(t, q_0). \quad (6)$$

The response of the system is integrated subject to the initial conditions in Eq. (5) and a variant on the algorithm in [16] is used to find the initial conditions, q_0 and period, T , that produce a periodic response. Then a psuedo-arclength continuation technique is used to predict a new solution and the process is repeated. As these solutions are continued to higher energy, additional linear modes may become active in the nonlinear response. Hence, the modal

amplitudes of all of the modes are estimated from the computed time response and are monitored as the shooting algorithm drives the system towards convergence. Additional modes are added to the coordinate set when their response becomes significant relative to the convergence tolerance. Hence, the number of linear modes in the modal coordinate set, here denoted m , increases with increasing energy. An outline of the NNM computation algorithm is provided below. The algorithm is essentially the same as that in [16] except for the fact that modal coordinates are used instead of physical coordinates, in order to reduce the size of the Jacobians required. The scheme used to augment the size of the modal coordinate set is also not present in their work.

- 1.) Provide an initial guess for the solution: $(q_{0,(0)}, T_{(0)})$
 - Begin the solution at a linear normal mode by setting one modal coordinate to a small value and set all other coordinates equal to zero. Use the linear natural frequency to determine the initial period, $T_{(0)}$.
- 2.) Correct the initial guess if necessary: $(q_{0,(1)}, T_{(1)})$
 - Use the scheme described in (3.b) to correct the initial guess. The first periodic solution that is found is denoted $(q_{0,(1)}, T_{(1)})$.
- 3.) Initiate the Predictor-Corrector Algorithm to compute the NNM solution branch: $(q_{0,(j)}, T_{(j)}) \quad j = 2, 3, \dots$
 - A predictor-corrector scheme computes the periodic solution branch to the nonlinear equations of motion, and must be initiated with a known solution $(q_{0,(1)}, T_{(1)})$.
 - a.) Prediction Step: $(q_{0\text{pr},(j+1)}, T_{\text{pr},(j+1)})$
 - The current solution $(q_{0,(j)}, T_{(j)})$ is used to find the trajectory of the solution branch to predict the next solution. A step-size controller, defined in [16], is used to determine the magnitude of the prediction step.
 - b.) Correction Step: $(q_{0,(j+1)}^{(k)}, T_{(j+1)}^{(k)})$
 - A Newton-Raphson iterative correction scheme is used to compute corrections $\Delta q_{0,(j+1)}^{(k)}$ and $\Delta T_{(j+1)}^{(k)}$ to the modal coordinates $q_{0,(j+1)}^{(k+1)}$ and period $T_{(j+1)}^{(k+1)}$. Throughout the correction iterations, the time histories of the response are transformed to modal coordinates and the modal amplitudes are monitored. Additional modes are considered to be important when their response at the end of the integration period is large relative to the convergence criterion, as explained subsequently. When this occurs the modal state vector $q_{0,(j+1)}^{(k)}$ is augmented by adding the next most influential mode.

Finite differences are used to compute the Jacobians needed for steps (2), (3.a) and (3.b) so that the approach can be coupled with existing finite element packages non-intrusively. (The algorithm of Peeters et al. achieves a cost savings by instead integrating the EOM and the analytically computed derivative of the EOM to obtain the Jacobian, but that derivative is not readily available in commercial software.) The details of the algorithm are presented in the following subsections.

A. Shooting Technique

The shooting technique is used to determine the periodic solutions of the nonlinear equation of motion described by Eq. (1). The approach solves the two-point boundary value problem [15], which is defined as

$$H(T, q_0) = z_T(T, q_0) - z_0(0, q_0) = \{0\} \quad (7)$$

The numerical algorithm is considered to have converged when the shooting function, $H(T, q_0) \in \mathbb{R}^{2N}$, satisfies the following tolerance.

$$\frac{\|H(T, q_0)\|}{\|z_0(0, q_0)\|} < \varepsilon \quad (8)$$

As in [16], the corrections used in the shooting technique are based on a Taylor series expansion of the nonlinear shooting function in Eq. (7). The corrections to the initial modal amplitudes and period ($\Delta q_0, \Delta T$) of the system are then found by solving the following overdetermined set of equations.

$$\begin{bmatrix} \frac{\partial H}{\partial q_0} \Big|_{q_0, T} & \frac{\partial H}{\partial T} \Big|_{q_0, T} \end{bmatrix} \begin{Bmatrix} \Delta q_0 \\ \Delta T \end{Bmatrix} = \{-H(T, q_0)\} \quad (9)$$

where the Jacobian is a $2N \times m+1$ matrix (it is assumed that $N \gg m$). It is computed using forward finite differences and hence its computation requires m integrations of the EOM over one period, T . The Moore-Penrose psuedo-inverse of the Jacobian can be used to compute ($\Delta q_0, \Delta T$) in a least squares sense. However, that approach proved unreliable in the examples that follow so instead H was also transformed into modal coordinates, reducing the size of the Jacobian from $2N \times m+1$ to $2m \times m+1$. This is accomplished using the transformation matrix,

$$B = \begin{bmatrix} \Phi_m^T M & 0 \\ 0 & \Phi_m^T M \end{bmatrix} \quad (10)$$

where B is a $2m \times 2N$ matrix, and the mode shape matrix Φ_m^T , contains the mode shapes of the active modes as its rows and M is the $N \times N$ mass matrix of the system. Premultiplying Eq. (9) by the transformation matrix B eliminates any portion of the shooting function that is orthogonal to the m modes in the active coordinate set, producing the following least squares problem,

$$\begin{bmatrix} \frac{\partial H_q}{\partial q_0} \Big|_{q_0, T} & \frac{\partial H_q}{\partial T} \Big|_{q_0, T} \end{bmatrix} \begin{Bmatrix} \Delta q_0 \\ \Delta T \end{Bmatrix} = \{-H_q(T, q_0)\} \quad (11)$$

where H_q represents the shooting function in terms of the m modal coordinates q_0 . Once the updates, ($\Delta q_0, \Delta T$), are found, the new initial states and periods are then given by the following.

$$q_0^{k+1} = q_0^k + \Delta q_0^k \quad (12)$$

$$T^{k+1} = T^k + \Delta T^k \quad (13)$$

This Jacobian defined in Eq. (11) is also used in the prediction and correction steps that follow.

B. Pseudo-Arclength Continuation: Prediction Step

The prediction step uses the latest computed solution $(q_{0,(j)}, T_{(j)})$ to compute a vector that is tangent to the NNM solution branch. The parameters, $(q_{0,(j)}, T_{(j)})$, are then updated by incrementing them a small amount in the tangent direction to obtain the first estimate of the $(j+1)^{\text{th}}$ solution, as detailed below. The prediction vector $\{P_{q,(j)}^T \quad P_{T,(j)}^T\}^T$ is computed by solving the linear system of equations defined by

$$\begin{bmatrix} \frac{\partial H_q}{\partial q_0} \Big|_{q_{0,(j)}, T_{(j)}} & \frac{\partial H_q}{\partial T} \Big|_{q_{0,(j)}, T_{(j)}} \end{bmatrix} \begin{Bmatrix} P_{q,(j)} \\ P_{T,(j)} \end{Bmatrix} = \begin{Bmatrix} 0 \\ 0 \end{Bmatrix} \quad (14)$$

where the Jacobian is computed as described previously. This requires m additional integrations of the equations of motion over the period T . The prediction vector is normalized to a unit length and the same step size control algorithm described by Peeters et al. is employed to obtain a prediction of the next period and initial modal amplitudes.

$$q_{0,pr,(j+1)}^{(1)} = q_{0,(j)} + s_{(j)} \cdot P_{q,(j)} \quad (15)$$

$$T_{pr,(j+1)}^{(1)} = T_{(j)} + s_{(j)} \cdot P_{T,(j)} \quad (16)$$

The step size controller, $s_{(j)}$, typically keeps the step size small enough so that only 2 to 5 iterations are necessary for the correction step to converge.

C. Pseudo-Arclength Continuation: Correction Step

The prediction of the modal state vector $q_{0,pr,(j+1)}$ and period $T_{pr,(j+1)}$ is evaluated for periodicity using the shooting function in Eq. (7). If the shooting function is not satisfied to the tolerance defined in Eq. (8), then a corrector step is initiated using the Newton-Raphson approach to compute an update to the modal amplitudes, $\Delta q_{0,(j+1)}^{(k)}$, and period $\Delta T_{(j+1)}^{(k)}$, where k denotes the k^{th} correction iteration. The updates are computed using the Jacobian matrix as shown in Eq. (11), augmented with the predictor vector in order to force the correction to be perpendicular to the predictor.

$$\begin{bmatrix} \frac{\partial H_q}{\partial q_0} \Big|_{q_{0,(j+1)}^{(k)}, T_{(j+1)}^{(k)}} & \frac{\partial H_q}{\partial T} \Big|_{q_{0,(j+1)}^{(k)}, T_{(j+1)}^{(k)}} \\ \{P_{q,(j)}\}^T & P_{T,(j)} \end{bmatrix} \begin{Bmatrix} \Delta q_{0,(j+1)}^{(k)} \\ \Delta T_{(j+1)}^{(k)} \end{Bmatrix} = \begin{Bmatrix} -H(T_{(j+1)}^{(k)}, q_{0,(j+1)}^{(k)}) \\ 0 \end{Bmatrix} \quad (17)$$

The updated period and initial conditions are then computed as in Eqs. (15) and (16).

The shooting function in Eq. (7) is evaluated at each correction iteration until convergence is met, at which point the converged modal state vector $q_{0,(j+1)}$ and period $T_{(j+1)}$ are stored and used to predict the next solution. As the energy increases, additional linear modes begin to contribute to the response of the nonlinear system. Or, in the event that the initial modal amplitude was already in the nonlinear region, additional modes may be needed when using shooting to obtain the first periodic solution $(q_{0,(i)}, T_{(i)})$. These modes, if not accounted for, may prevent the correction step from converging. To circumvent this, the following procedure is used to detect modes that are important in the response and to add them when appropriate. Notice that, since the size of the Jacobian required in Eq. (17) above is governed by the number of active modal coordinates, it is preferable to include the smallest number of modes possible.

D. Add Linear Modal Coordinate

At each correction iteration, the following procedure is used to determine when the shooting function H has significant contributions from modal coordinates that are not included in the reduced coordinate set q_0 . The shooting function is premultiplied by the transformation matrix defined by Eq. (10) to eliminate the contributions of modes that are not in the active coordinate set and then transformed back to physical coordinates, as follows.

$$\hat{H} = \begin{bmatrix} \Phi & 0 \\ 0 & \Phi \end{bmatrix} [B] \{H(T_{(j+1)}^{(k)}, q_{0,(j+1)}^{(k)})\} \quad (18)$$

This new shooting function, $\hat{H} \in \mathbb{R}^{2N}$, contains only the contributions of the active modal coordinates to the shooting function, H . Hence, the contribution of the other modal coordinates is $H - \hat{H}$. When $H - \hat{H}$ is a large fraction of H , the neglected modes may prevent convergence. Hence, the following tolerance is used to determine when a new modal coordinate is needed.

$$\frac{\|H - \hat{H}\|}{\|H\|} < \varepsilon_{add} \quad (19)$$

If the tolerance ε_{add} is not satisfied, then the modal amplitudes of all of the modal coordinates are computed using

$$q(t) = [I \quad 0][B]\{z(t, q_{0,(j+1)}^{(k)})\} \quad (20)$$

and the largest modal coordinate that is not already in the set q_0 is added to the modal coordinate set. The correction procedure is then resumed with m augmented by one. It should be noted that this procedure may add modes to the coordinate set that aren't needed to satisfy convergence, for example a prediction far from the solution may excite other modes that disappear once convergence is reached. However, the prediction step is typically kept very small so that only two or three iterations are needed in the correction step, and one would hope that unnecessary modes would not be significantly excited so close to the solution branch.

E. FEA-Interface with NNM Algorithm

The NNM algorithm described above has been implemented in MATLAB®. This section describes the interface used to connect the continuation routine to a nonlinear FEA package. A schematic of this interface is shown in Fig. 1. A structural model is constructed in an existing FEA package that accommodates large displacements. (Other nonlinearities, such as contact elements and material nonlinearity are also readily accommodated, although this was not explored here.) The initial conditions, z_0 , are supplied to the model by MATLAB and integrated over a desired period T using the available time integration schemes. Once the response has been computed, the time histories can be exported to MATLAB for post-processing of the response (e.g. determining whether q_0 and T satisfy the shooting function). Since most commercial nonlinear FEA packages are capable of handling geometric nonlinearities, this approach could be applied to a variety of packages. The results presented in this work utilize the ANSYS® nonlinear transient solver.

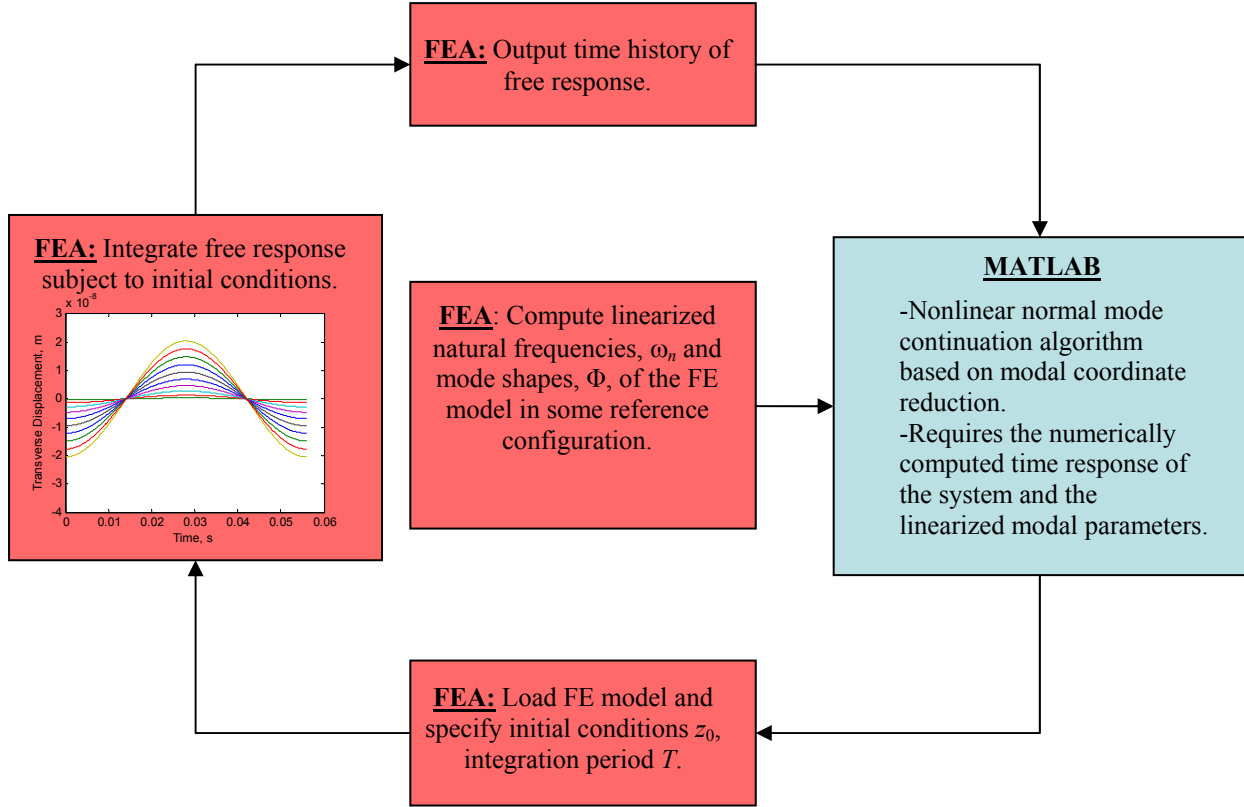


Figure 1. Interface between NNM algorithm and nonlinear FEA package.

As mentioned previously, this method will be referred to as the full-modal continuation method (FMCM), and will be taken as the truth model in this work as the solutions that it produces always produce a periodic response of the full FEA model. In the next section, a method for computing a reduced order model of a geometrically nonlinear structure is reviewed. The nonlinear normal modes of these reduced order models can be computed directly using the same methodology described above. However, since these models are already quite small the reduction procedure described above is not used but instead all of the available degrees of freedom are included in q_0 . Hence, the algorithm used to find the NNMs of these ROMs is the same as that presented by Peeters et al. [16].

III. Computation of NNMs using Reduced Order Models

In the past decade, many methods for constructing Reduced Order Models (ROMs) for nonlinear systems have been developed. By truncating high frequency modes, ROM methods reduce a finite element model to a low-order system of nonlinear equations that govern the amplitudes of the linear modal coordinates of the structure [19]. In previous work ([20],[1],[22]), these nonlinear modal equations were integrated in time to predict the response of the structure. For our application, the closed form nonlinear modal equations will be used to find the NNMs of the system.

A. ROM Theory

Consider a linear, undamped multiple DOF system. The equations of motion are of the form

$$M\ddot{x} + Kx = F \quad (21)$$

where M and K represent the linear mass and stiffness matrices, respectively, x corresponds to N physical DOFs of the system, and F is the external force applied to the system. The homogeneous form of Eq. (21) is used to find the linear mode shapes (eigenvectors) Φ . The mode shapes are mass normalized, so substituting Eq. (2) into Eq. (21) and pre-multiplying by Φ^T yields the uncoupled equation of motion for the r^{th} mode,

$$\ddot{q}_r + \omega_r^2 q_r = \Phi_r^T \mathbf{F} \quad (22)$$

where ω_r is the linear natural frequency of the system, and q_r is the modal amplitude. A set of N_r uncoupled equations for some subset of the system's modes defines a linear reduced order model for the system. In the following the coordinates of the retained modes will be denoted $[q_1, q_2, \dots, q_{N_r}]$ where $N_r \ll N$. If the system is nonlinear, then nonlinear forces will affect each mode's response and couple it to the other modal coordinates. This is accounted for by adding a nonlinear stiffness term f_{NL} to Eq. (22).

$$\ddot{q}_r + \omega_r^2 q_r + f_{NL}^r(q_1, q_2, \dots, q_{N_r}) = \Phi^T \mathbf{F} \quad (23)$$

Notice that f_{NL} for the r^{th} equation is expressed as a function of N_r different modal amplitudes, which correspond to all of the modes in the truncated linear mode set. Therefore, the nonlinear modal equations are coupled by the nonlinear force terms. For the r^{th} mode, the nonlinear force is approximated by polynomial model,

$$f_{NL}^r(q_1, q_2, \dots, q_{N_r}) = \sum_{i=1}^{N_r} d_i^r q_i + \sum_{i=1}^{N_r} \sum_{j=1}^{N_r} a_{ij}^r q_i q_j + \sum_{i=1}^{N_r} \sum_{j=1}^{N_r} \sum_{k=1}^{N_r} b_{ijk}^r q_i q_j q_k \quad r = 1, 2, \dots, N_r \quad (24)$$

where the nonlinear stiffness coefficients are represented by d (linear), a (quadratic), and b (cubic) terms. For example, if $N_r=1$ the second summation reduces to $a_{11}^1 q_1^2$ and the third summation to $b_{111}^1 q_1^3$. For the beam model studied in Section V, these terms capture the nonlinear stiffening or softening effects that arise due to large deflections in the beam.

The nonlinear stiffness coefficients from Eq. (24) have been found in a variety of ways. Two methods for solving the nonlinear stiffness coefficients were explored in this work. The first method was first presented by McEwan [20] and is referred to as the applied loads procedure in [19] or as Implicit Condensation (IC) in [1]. The second method is described by Muravyov and Rizzi in [21] and is referred to as the enforced displacements procedure in [19]. In both cases, the same finite element package described previously is used to solve nonlinear static problems to calculate either the nonlinear reaction forces when displacements are enforced, or the nonlinear displacements when loads are applied to the FEA model.

B. Applied Loads Procedure

In order to obtain the nonlinear stiffness coefficients with the applied loads procedure, a series of nonlinear static solutions are found with prescribed loads. For each solution, the applied load vector is a scaled linear combination of the linear mode shapes as

$$\mathbf{F} = M (sf_1 \Phi_1 + sf_2 \Phi_2 + \dots + sf_N \Phi_N) \quad (25)$$

The scaling factors sf can be varied to exercise the desired amount of nonlinearity in the structure. Note that many of the previous works on the applied loads method did not necessarily use the mass matrix as shown above when computing the load vector, but it is needed to obtain a valid force profile for a linear system. Although not discussed in detail, Gordon and Hollkamp [1] used a similar approach in which the force, \mathbf{F} , was the reaction force (computed by the *linear* FEA solver) required to obtain the displacement $x = (sf_1 \Phi_1 + sf_2 \Phi_2 + \dots + sf_2 \Phi_2)$.

Once displacements are obtained from each of the static load cases, a least squares approach is used to find the nonlinear stiffness coefficients. For further information on this method see [20]. One major advantage of the applied loads procedure is that it implicitly captures membrane displacements and essentially softens the ROM [1].

C. Enforced Displacements Procedure

The enforced displacements procedure also uses a series of nonlinear static solutions to find the ROM. However, in this method the displacement is prescribed and the nonlinear FEA solver computes the reaction force required to hold the structure in that deformed shape. For example, a multi-modal displacement can be written as

$$\mathbf{X} = q_1 \Phi_1 + q_2 \Phi_2 + \dots + q_N \Phi_N \quad (26)$$

and the FEA software returns the reaction force which is a sum of modal contributions that satisfies

$$\omega_r^2 q_r + f_{NL}^r(q_1, q_2, \dots, q_N) = \Phi^T \mathbf{F} \quad (27)$$

where \mathbf{F} is the reaction force required to hold the structure in equilibrium.

One other advantage of this method is that it allows one to circumvent the least squares problem used to find the coefficients in Eq. (24). Instead, the nonlinear stiffness coefficients can be found using algebraic relations if a special pattern of applied modal displacements is used [22], although this procedure was not implemented in this work. One disadvantage of this method is that membrane displacements can only be captured if membrane modes are explicitly included in the modal basis [19].

IV. Numerical Results

A. 11DOF Spring-Mass System

In order to validate the full-modal continuation method (FMCM), the spring-mass system shown in Fig. 2 was used. Each mass is connected to its neighbors (or ground for the masses on the ends) by both a linear spring and a cubic spring with coefficient k_{nl} . The following values are used for the linear spring constants, which is equivalent to nondimensionalizing the problem by defining time such that the period of a single oscillator would be 2π : $k=1$, $m=1$, and $k_{nl}=1$.

The first three NNMs of the system were found using the FMCM algorithm and are displayed on the frequency-energy plot in Fig. 3. The tolerances for the periodicity condition and mode addition criterion were $\epsilon=10^{-6}$ and $\epsilon_{add}=0.1$, respectively. At low energies, each NNM is initiated at a linear normal mode (LNM) shape and frequency.

The numbers near each line indicate the energy level at which additional modal degrees-of-freedom were added to the coordinate set by the algorithm described previously. The results show that, as energy increases, the nonlinearity in the system becomes important and additional LNMs are needed in order to obtain a solution that satisfies the shooting function. For example, for the first NNM curve, the 3rd LNM is added at approximately $E = 2 \cdot 10^{-5}$ and the 5th, 7th, 9th and 11th all enter when $0.003 < E < 0.07$. With all of the odd LNMs added, the algorithm is then able to compute this NNM out beyond the point at which the natural frequency has increased by a factor of five.

It is surprising that so many LNMs (essentially half) are required for the first NNM. Of course, in many applications the frequencies change by

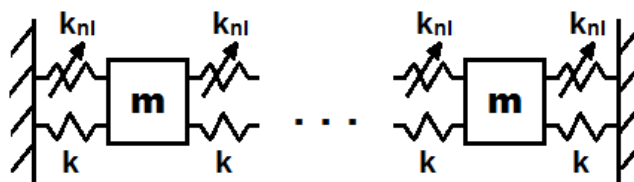


Figure 2. 11DOF lumped mass system with cubic nonlinearities.

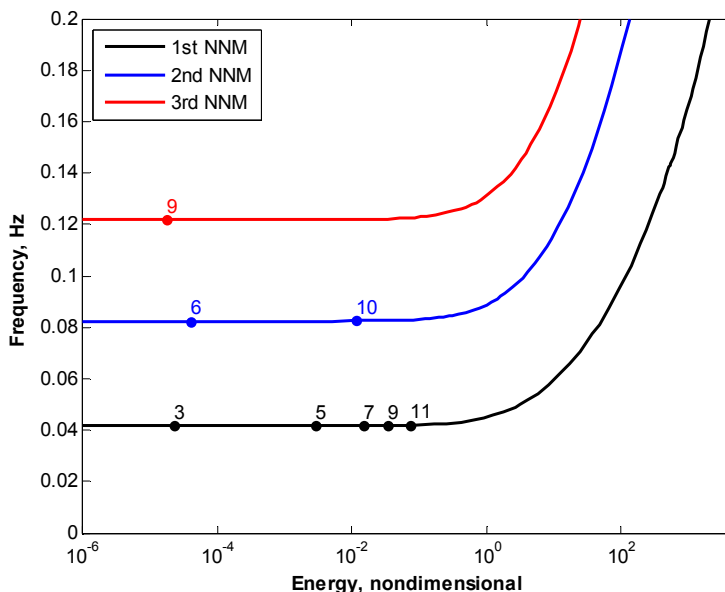


Figure 3. Frequency vs. Energy for the first three NNMs of an 11DOF lumped mass system.

only a few tens of percent, but in this example half of the structure's LNMs were needed to advance even to the point where the natural frequency of the system had changed by just one percent.

In Table 1, the number of one-period integrations required to obtain NNMs in Fig. 3 is compared to the result when the authors' implementation of the full algorithm in [16] is used. For each NNM, the modal method requires far fewer calls to the integration routine. By truncating the coordinates to dynamically important LNMs, the computational cost is decreased by 45 to 76%, or by a factor of between $\frac{1}{2}$ and $\frac{1}{4}$.

Table 1. Comparison of the number of one-period integrations required to obtain the NNM curves in Figure 3.

NNM curve	# Integrations using Full Order Solution	# Integrations using Modal Continuation Method	Percent Change (%)
1	5810	3156	-45
2	1478	427	-71
3	1370	324	-76

For the first NNM curve, the odd LNMs are added in the order of increasing energy and it was thought that this would be the case for all NNM curves. However, for the second NNM curve, the 6th LNM is added at approximately $E = 4 \cdot 10^{-5}$ followed by the 10th LNM

added at $E = 0.01$. For the third NNM curve, the 9th LNM is added at approximately $E = 2 \cdot 10^{-5}$. If a system with a larger number of masses is considered a pattern evolves for the addition of LNMs as seen in Table 3. For each NNM, the LNMs are added in a sequence defined by the number of the linear mode at which the NNM originates multiplied by the set of odd numbers, $\{3, 5, 7, 9, \dots\}$. This sequence is due to the similarities in shape of the LNMs to the associated NNM and would only apply to this particular system.

The number of modes required to achieve convergence depends on both the continuation convergence tolerance, ϵ , and on the amplitude ratio, ϵ_{add} , at which additional modes are added. Table 2 compares the effect of these settings on the algorithm and the resulting computational cost required to compute the first NNM until the frequency has increased by more than a factor of 2.

Table 3. Addition sequence of LNMs.

NNM curve	1 st LNM	2 nd LNM	3 rd LNM	4 th LNM	...
1	3	5	7	9	...
2	6	10	14	18	...
3	9	15	21	27	...
\vdots	\vdots	\vdots	\vdots	\vdots	\ddots

Table 2. Effect of varying ϵ_{add} and ϵ on the frequency at which each LNM is added when computing the 1st NNM curve. The computational cost is also shown, described by the number of 1-period integrations required to reach 0.1 Hz.

ϵ_{add}	ϵ	Percent Shift in 1 st NNM Frequency when each LNM is Added					# Integrations to reach 0.1 Hz frequency
		3 rd LNM	5 th LNM	7 th LNM	9 th LNM	11 th LNM	
10^{-8}	10^{-6}	0.00021	0.027	0.061	0.14	0.31	892
10^{-4}	10^{-6}	0.00021	0.027	0.061	0.14	0.31	892
0.01	10^{-6}	0.00021	0.027	0.14	0.31	0.69	883
0.1	10^{-6}	0.00021	0.027	0.31	0.69	0.69	881
0.1	10^{-4}	0.010	0.31	0.69	1.53	2.29	671
0.1	0.01	2.19	2.19	3.77	3.77	3.77	480
0.1	0.1	24.86	N/A	N/A	N/A	N/A	272

Table 2 shows that the amplitude ratio, ϵ_{add} , does not strongly influence the algorithm although it must be set less than 1 or the algorithm may fail to converge. In this example, the continuation algorithm always seems to add LNMs at about the same frequency shift no matter what the value of ϵ_{add} . On the other hand, the convergence tolerance, ϵ , can drastically reduce the computational cost. Increasing the tolerance from 10^{-6} to 10^{-2} reduces the number of integrations by more than one half for this 11DOF system, and the frequency energy dependence still tends to be captured quite accurately (at least for this case where no internal resonances occur). However, this also reduces the

accuracy of the solutions that are obtained and may also reduce the accuracy of the finite difference gradients causing the algorithm to diverge.

Now consider the effect of asymmetry on the modal continuation routine. An asymmetric system was created by removing all of the nonlinear springs except the one between the first mass and ground. The first NNM was found using the modal continuation method and is displayed on the frequency-energy plot in Fig. 4. The parameters used were $\epsilon = 1 \cdot 10^{-4}$ and $\epsilon_{\text{add}}=0.1$. The result shows that all of the LNMs of the system were needed to reach a frequency shift of a few percent. The nonlinear spring breaks the symmetry of the system causing the symmetric and anti-symmetric modes to all participate. It is also interesting to note that an internal resonance appears once the frequency has shifted about ten percent. The second and third NNMs were also computed (not shown) revealing a similar trend. With all of the LNMs added, the algorithm can compute the NNMs but the cost required to compute the higher energy part of the curve is no less than that of the algorithm of Peters et al.

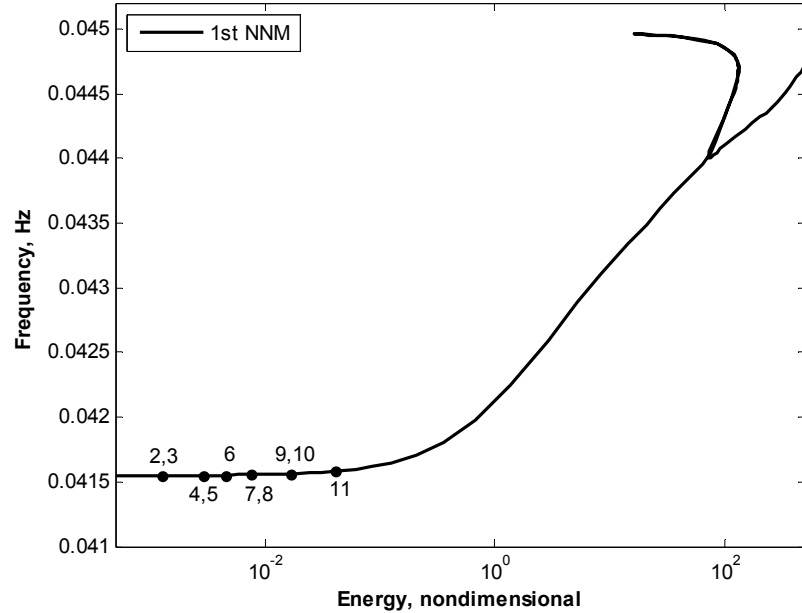


Figure 4. Frequency vs. Energy for the first NNM of an asymmetric 11DOF lumped mass system.

B. Beam with Geometric Nonlinearity

Next, the FMCM algorithm was applied to a finite element model (FEM) of a one-dimensional clamped-clamped beam with geometric nonlinearity. The FEM has ten 2-node *beam3* elements, resulting in a total of 27 DOF. The model geometry is adopted from [1, 19, 23], where the beam was used as a benchmark to test a variety of nonlinear model reduction strategies. The beam is 9 inches long, 0.5 inch wide and 0.031 inch thick. It is constructed of steel with a Young's modulus of 29,700 ksi, a shear modulus of 11,600 ksi and a mass density of $7.36 \cdot 10^{-4}$ lb-s²/in⁴. Large deformation analysis of the flat, thin beam exhibits stiffening nonlinearities in its elastic range as the amplitude of the displacement increases. The stiffness depends nonlinearly on the response due to the coupling between the axial and transverse displacements.

The first 3 nonlinear normal modes of the beam model were computed using the FMCM approach with $\epsilon=10^{-4}$ and $\epsilon_{\text{add}}=0.1$. The solution branches are shown in Fig. 5 where the frequency is plotted along the vertical axis and maximum physical displacement of an appropriate node (mid point for NNMs 1 and 3, and quarter point for NNM 2) on the horizontal axis. Each solution branch is initiated at a single linear modal response at low amplitude. The full, mass normalized mode matrix is directly computed in ANSYS with a block Lanczos solver and is used to transform the coordinates from physical displacements (x_0) to modal displacements (q_0). At each step in the algorithm the free response to an applied initial condition (q_0) was directly integrated using the implicit Newmark-Beta scheme in the nonlinear full order transient analysis. The average acceleration method was used with integration parameters $\gamma=0.5$ and $\beta=0.25$ [24], such that algorithmic damping is not introduced into the time response. A suitable step size is required for a nonlinear dynamic simulation to accurately capture the higher order harmonics of the response. For the results shown, 1,000 equidistant time steps are used over one period of integration.

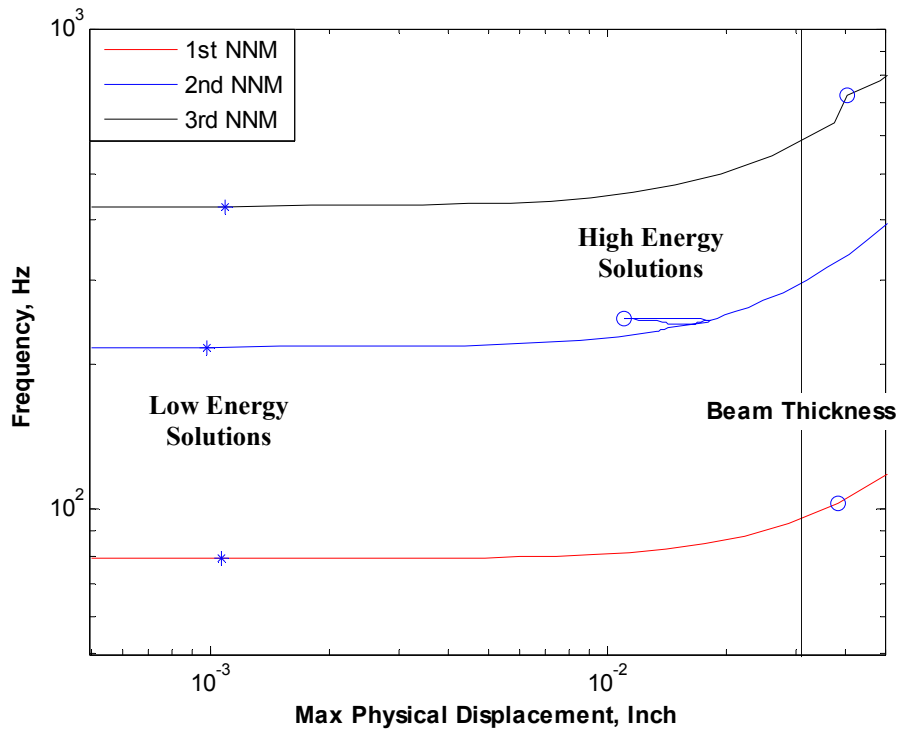


Figure 5. Frequency vs. Max Physical Displacement of nonlinear normal modes (1 through 3) of a geometrically nonlinear beam.

The nonlinear normal mode solutions are computed out to a relatively large shift in frequency, between 50 to 85%. This approximately corresponds to the range of nonlinearity observed in the application of interest [1, 19, 23]. Two specific solutions are marked on the branches in Fig. 5, namely low energy solutions (*) and high energy solutions (o). All of the required modes in the modal coordinate set were all added before reaching the points marked with stars (*) in Fig. 5. There has not yet been any appreciable shift in frequency at this point, so it is surprising that so many modes are needed to advance to this point. This is similar to the results seen with the 11DOF model. Each of the modal coordinates needed in the set q_0 for each NNM branch are listed in Table 4, along with the linearized natural frequencies. The table also gives the maximum frequency shift of each mode, expressed as a percentage of the original linear natural frequency. Because this system is planar, the linear normal modes can be readily characterized as either axial modes ($\{16, 20, 21, 22, 23, 24, 25, 26, 27\}$), symmetric bending modes ($\{1, 3, 5, 7, 9, 11, 13, 15, 18\}$) or asymmetric bending modes ($\{2, 4, 6, 8, 10, 12, 14, 17, 19\}$). Hence, it appears that the first nonlinear normal mode requires all of the symmetric bending modes to be included in the modal coordinate set, and all of the asymmetric axial modes ($\{20, 22, 24, 26\}$). The second NNM similarly requires all of the asymmetric bending modes and asymmetric axial modes. For all three cases, 13 of the 27 modal coordinates are needed to compute the NNM branches, corresponding to a factor of two reduction in the size of the Jacobians needed in the continuation algorithm.

Table 4. Results of FMCM NNM Solutions

NNM Solution	Linearized Frequency (Hz)	% Frequency Shift	Additional Mode Order	Number of Prediction Steps
1	78.9	55.0	{1, 20, 22, 3, 24, 26, 5, 7, 9, 11, 18, 13, 15}	21
2	217.7	67.7	{2, 22, 20, 24, 26, 4, 6, 8, 10, 17, 12, 14, 19}	65
3	426.9	82.3	{3, 20, 24, 26, 22, 5, 1, 7, 9, 15, 11, 18, 13}	20

The shapes of the NNMs at the points marked (*) and (o) are shown in Fig. 5. Plots 6a through 6c show the displacement of the beam that initiates the periodic orbits. Each initial displacement has been normalized so the deformation shape is more easily compared. The dashed blue line corresponds to the NNM at low energy (points marked with ‘*’ in Fig. 5) and the solid red line represents the NNM at high energy (points marked with ‘o’). At low energy, the initial displacements are very similar to the linearized mode shape of the beam, but as energy is increased, the initial displacement shapes begin to evolve. The second NNM shape begins as the shape of the 2nd linearized mode and evolves into the shape of the 4th linearized mode. This occurs as a 3:1 internal resonance is reached at this energy level, causing the 2nd and 4th modes to interact. In contrast, the first and third NNMs still have approximately the same shape at high energy, even though their natural frequencies have shifted 20% and 70%, respectively.

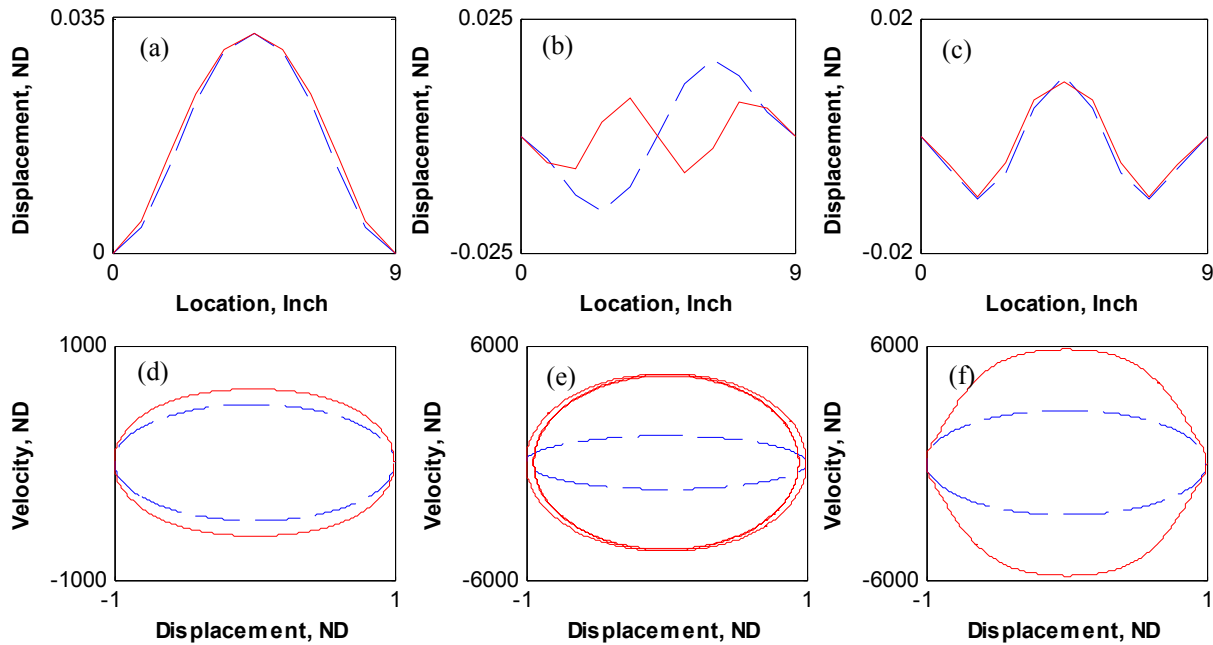


Figure 6. Initial displacements of the beam for the low and high energy solutions shown in Fig. 5 for NNMs 1, 2 and 3 respectively (a to c). Phase portraits of periodic orbits for a reference node for the same low and high energy solutions (d to f). Dashed lines correspond to the low energy solutions and solid lines to the high energy solutions.

The phase portraits shown represent the transverse displacement and velocity of the node with the largest displacement. The shape of the orbit reflects the importance of higher harmonics and gives insight into the degree of nonlinearity present in the response. The phase portraits are normalized to unit maximum displacement, so widening of the phase portrait in the vertical direction (velocity) reflects a stiffening nonlinearity. The effect of nonlinearity is especially notable in the 3rd NNM, where the shape of the orbit is far from round at high energy; the points of maximum displacement almost has the character of an impact, with the initial velocity changing from positive to negative over a short interval.

The number of prediction steps per NNM branch are presented in Table 4. These provide a measure of computational effort required for each curve. Each solution along the branch has one prediction step, and k correction steps and each one of those steps requires an evaluation of a Jacobian. For the first mode there were 13 modal DOF over most of the curve so this required 13 nonlinear transient solutions. The first and the third NNMs require 21 and 20 predictions, respectively, but the second curve required three times as many. This occurs because the algorithm must take smaller steps to trace out the internal resonance in the 2nd NNM. The step size controller sets the magnitude of the predictor step based on the number of corrections and an optimal value set by the user. The step size is either increased or decreased depending on how many steps are required to converge on the solution.

This application has shown that the FMCM method can compute the NNMs of a structure modeled in finite element software without any a priori information about the modes that are needed; the algorithm automatically adds

those modes that are needed for convergence. Unfortunately, the cost of the approach is still quite high as only a factor of 2 reduction was realized. In the next section the reduced order modeling methods are used to compute the first NNM of the beam and the result is compared with the FMCM to evaluate the accuracy of the ROMs.

V. Using Reduced Order Models to Compute Nonlinear Normal Modes

The two ROM procedures, implicit condensation (IC) and enforced displacements, were used to find the frequency-displacement dependence of the 1st NNM using the same finite element model described in Section IV. For both ROMs, only the first symmetric bending mode was used in computing one nonlinear equation of motion. This equation contains nonlinear stiffness coefficients d (linear), a (quadratic), and b (cubic), with the linear stiffness coefficient equal to the linearized natural frequency squared, so $d = \omega_1^2$. The quadratic and cubic stiffness coefficients were curve fit using a least squares approach. The tolerance for the periodicity condition was set to $\epsilon=10^{-6}$ and the resulting NNM curves are shown in Fig. 7.

Preliminary studies revealed that the scaling and quantity of load/displacement cases was critical to the quality of the ROM. If the applied load/displacement was too small then the nonlinearity was not captured and the curve fit used to find the nonlinear coefficients would be ill conditioned. The guidelines from [1] were used in this work, specifically that the load/displacement used to obtain the ROM produced a displacement on the order of the beam thickness. Hence, one would expect the NNM curves in Fig. 7 to be accurate below 0.031 inches maximum displacement but beyond that point the force displacement relationship represents an extrapolation and may not be accurate. In any event, higher displacement levels may require higher order polynomial terms, but this is not typically done (see, e.g. [1]), since the number of terms to identify increases geometrically.

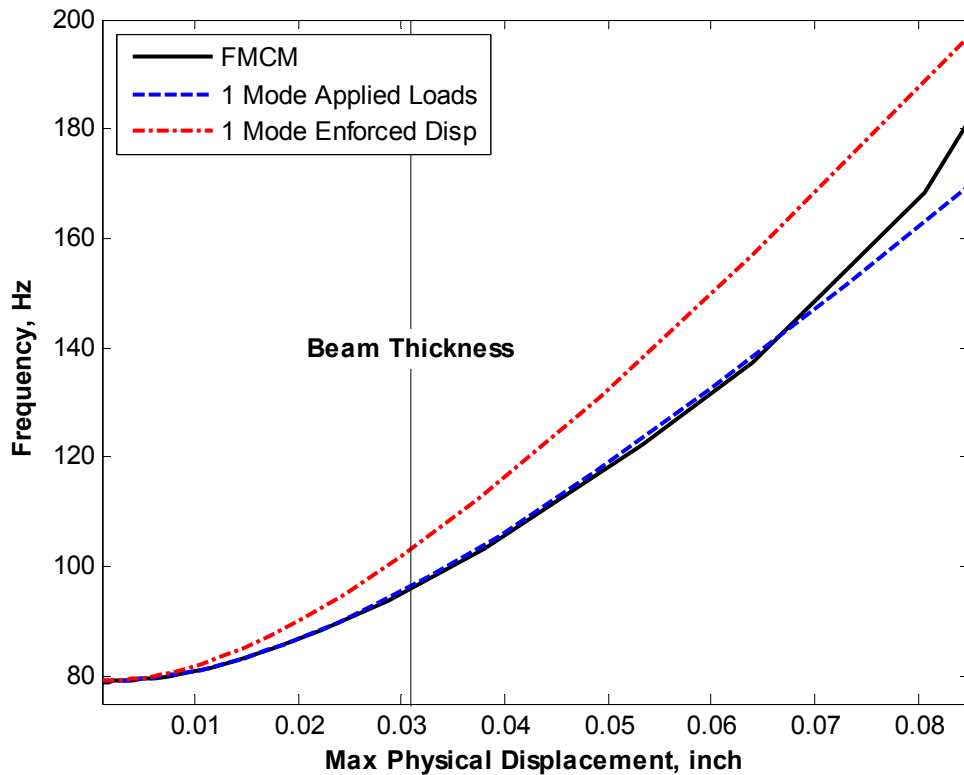


Figure 7. Frequency vs. maximum displacement of the center point of the beam for the 1st NNM computed from the full finite element model (FMCM method) and two reduced order models.

The results show that the applied loads model captures the true frequency-energy dependence of the system out to more than twice the thickness of the beam, even with only one mode used in its construction. In contrast, the

enforced displacement method produces a NNM that is quite a bit stiffer than the true NNM. For straight beams such as this the enforced displacement method is known to require that the axial modes be included in the ROM to provide accurate results [1], and the model used to generate Fig. 7 only included the first symmetric bending mode. In contrast, the applied loads method implicitly captures the softening effects of all of the modes; the load that is used to generate it satisfies static equilibrium of the full-order model. Either of these methods represents a huge reduction in computational effort relative to the FMCM algorithm, since one need only compute a few nonlinear static solutions and then find the NNMs of an SDOF equation of motion. It should also be noted that, while these methods predict the frequency-energy (or frequency-displacement) dependence of the NNM, since they are formulated based on a single mode they do not allow one to predict the change in the deformation shape of the NNM with increasing energy.

In practice a full order solution, such as that provided by FMCM, might not be available. In that case one should test the convergence of the ROM by increasing its order and recomputing the NNMs. Otherwise the accuracy of the results is not established and

important features, such as the internal resonance shown in Fig. 5, might be missed. This is demonstrated in Fig. 8, where the FMCM solution is compared with various multi-mode IC models. ROMs that include various numbers of

Table 5. Details Regarding Multi-Mode ROMs

Mode Set	Number of Load Cases	Number of Polynomial Coefficients per Mode	Max Percent Error in Frequency
{1}	2	2	0.43 %
{1 3}	8	7	0.12 %
{1 3 5}	18	16	0.05 %

symmetric bending modes: {1}, {1 3}, and {1 3 5} are compared to the FMCM result. The number of load cases and number of polynomial coefficients for each modal set can be seen in Table 5. Also, for displacements up to the thickness of the beam, the maximum percent error in the estimated NNM frequency is shown (based on the difference between the ROM frequency and the FMCM solution) to gauge the accuracy of the ROMs. As expected, the frequency predicted by the ROM becomes more accurate as the number of modes is increased, although it is already quite accurate even for the one-mode model. Figure 8 shows that the ROM also estimates the NNM curve more accurately for displacements greater than the beam thickness as the order is increased. It should be noted, however, that for even larger displacements the convergence was somewhat erratic. For example, the {1 3} ROM predicts an internal resonance a little beyond the region shown which is not present in the prediction from the {1 3 5} ROM.

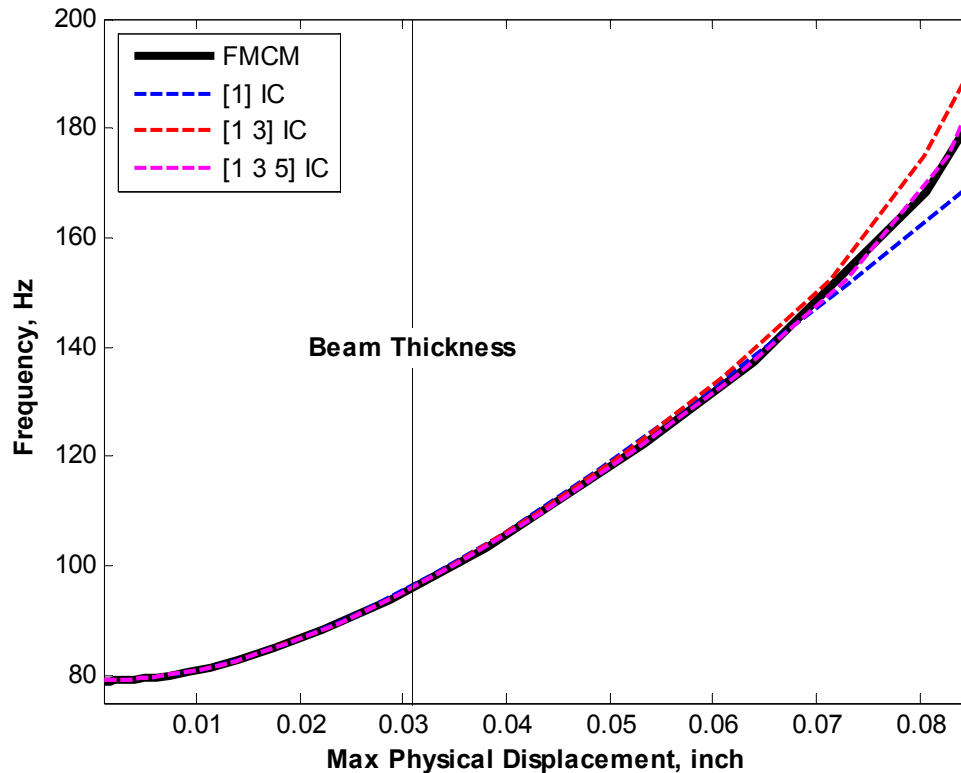


Figure 8. Frequency vs. maximum displacement of the center point of the beam for the 1st NNM for various multi-mode IC models. The NNM computed by FMCM is also shown for reference.

VI. Conclusions

This work presented a variation on the continuation technique developed by Peeters et al. [16] to enable the computation of nonlinear normal modes for geometrically nonlinear structures modeled in commercial finite element software. The Jacobians required were computed with finite difference gradients, since the analytical derivative of the equations of motion was not available, and a reduction based on the linear modes was used to reduce the size of the required Jacobians. The proposed method was evaluated first using a simple 11-DOF spring mass system and then using a 10-element model of a fixed-fixed beam. The proposed approach was found to reduce the number of one-period integrations required to compute the NNMs by a factor of between two and four, although larger reductions were possible if one could tolerate larger errors in the predicted NNM. While this represents a significant reduction in computation, it is surprising that such a large number of modes are needed to allow the numerical continuation scheme to converge. Furthermore, most of the computational savings that were realized came about due to symmetries in the system, which could have been exploited when creating the finite element model to achieve even more significant computational savings.

The FMCM method was also compared with two reduced order modeling approaches, and these comparisons seem to explain why the FMCM method required so many modes to estimate the NNMs. The model reduction employed by the FMCM is analogous to the enforced displacement ROM. In either case the motion of the actual structure is described as a superposition of the linear modes. In Fig. 7 this was found to result in an overly stiff model and convergence is quite slow as linear modes are added to the model. (This feature was not illustrated for the enforced displacement ROM, but analogous behavior is seen in Fig. 8 for the applied loads ROM.) Hence, since the FMCM method seeks to drive the solution of the FEA model to a periodic limit cycle with a relatively low tolerance ($\epsilon=10^{-4}$ in most of these examples), quite a large number of linear modes is needed. In any event, the FMCM algorithm does provide insight into which linear modes of the structure are dynamically important to each NNM. This information is valuable for many reasons and could merit the computational expense. In future works, more

complicated geometries will be evaluated in order to further validate this approach and to see whether the reduction in cost is larger for a more complicated system.

Two ROM methods were also explored and found to provide a very attractive alternative to the FMCM method, especially the applied loads ROM, which was found to accurately predict the frequency-energy dependence of the first NNM over the displacement range of interest even when only one mode was used. However, that method has some important limitations as well. The ROMs should be computed with various sets of linear modes to assure that convergence has been obtained and that any internal resonances have been captured, but the cost required to compute the ROMs goes up dramatically with increasing model order. For example, according to Gordon & Hollkamp [1] the number of nonlinear polynomial coefficients in a ROM increases from only two for a single degree of freedom ROM to between 935 and 2750 for a 10-DOF ROM depending on how it is calculated. Hence, a large number of static load cases may be needed to compute the ROM and there is an increased likelihood of ill-conditioning in the curve fit making the model difficult or impossible to estimate. Furthermore, one does not know a priori which linear modes should be included in the ROM to estimate a given set of NNMs. Also, one commonly mentioned fault of reduced order models is that they tend to be specific to the loading case for which they were derived. Although not shown in this paper, the ROM for the beam was initially created using displacements that were about 16 times the beam thickness. That led to quite unsatisfactory results as both ROMs were overly stiff at small displacements (recall that the order of the polynomials was fixed). This also led to non-intuitive results as the model order was increased with the NNM estimated by the ROM stiffening rather than softening as additional linear modes were added to the ROM.

Despite these challenges, it would be very attractive to have a ROM that was known to accurately capture several NNMs of a system. The NNMs capture the fundamental periodic solutions of the nonlinear system and form the backbones of its nonlinear frequency response. Hence a model that captures a set of relevant NNMs accurately might be more likely to reproduce the behavior of a system in a range of environments. Similarly, a comparison between the true system's frequency-energy plot and the frequency-energy plot of the ROM might be far more informative and comprehensive than a comparison of their transient responses (which is what is seen most commonly in the literature). These ideas should be explored more fully in future works.

Acknowledgments

This work was supported by the Air Force Office of Scientific Research, Award # FA9550-11-1-0035, under the Multi-Scale Structural Mechanics and Prognosis program managed by Dr. David Stargel.

References

- [1] R. W. Gordon and J. J. Hollkamp, "Reduced-Order Models for Acoustic Response Prediction," Air Force Research Laboratory (AFRL), Wright-Patterson Air Force Base, OH AFRL-RB-WP-TR-2011-3040, 2011.
- [2] D. J. Segalman, "A Four-Parameter Iwan Model for Lap-Type Joints," *Journal of Applied Mechanics*, vol. 72, pp. 752-760, September 2005.
- [3] D. J. Segalman, "Model reduction of systems with localized nonlinearities," *Transactions of ASME. Journal of Computational and Nonlinear Dynamics*, vol. 2, pp. 249-66, 2007.
- [4] A. J. Culler and J. J. McNamara, "Coupled Flow-Thermal-Structural Analysis for Response Prediction of Hypersonic Vehicle Skin Panels," in *51st AIAA/ASME/ASCE/AHS/ASC Structures, Structural Dynamics, and Materials Conference*, Orlando, Florida, 2010.
- [5] R. D. Blevins, I. Holehouse, and W. R. Wentz, "Thermoacoustic Loads and Fatigue of Hypersonic Vehicle Skin Panels," *Journal of Aircraft*, vol. 30, p. 971 to 978, 1993.
- [6] R. M. Rosenberg, "Normal modes of nonlinear dual-mode systems," *Journal of Applied Mechanics*, vol. 27, pp. 263-268, 1960.
- [7] A. F. Vakakis, "Non-linear normal modes (NNMs) and their applications in vibration theory: an overview," *Mechanical Systems and Signal Processing*, vol. 11, pp. 3-22, 1997.
- [8] G. Kerschen, M. Peeters, J. C. Golinval, and A. F. Vakakis, "Nonlinear normal modes. Part I. A useful framework for the structural dynamicist," *Mechanical Systems and Signal Processing*, vol. 23, pp. 170-94, 2009.
- [9] A. F. Vakakis, D. M. McFarland, L. Bergman, L. I. Manevitch, and O. Gendelman, "Isolated Resonance Captures and Resonance Capture Cascades Leading to Single- or Multi-Mode Passive Energy Pumping in Damped Coupled Oscillators," *Journal of Vibration and Acoustics*, vol. 126, pp. 235-244, 2004.
- [10] N. Boivin, C. Pierre, and S. W. Shaw, "Non-linear normal modes, invariance, and modal dynamics approximations of non-linear systems," *Nonlinear Dynamics*, vol. 8, pp. 315-346, 1995.

- [11] C. Pierre, D. Jiang, and S. W. Shaw, "Nonlinear normal modes for vibratory systems under harmonic excitation," *Journal of Sound and Vibration*, vol. 288, pp. 791-812, 2005.
- [12] P. Apiwattanalunggam, S. W. Shaw, and C. Pierre, "Component mode synthesis using nonlinear normal modes," *Nonlinear Dynamics*, vol. 41, pp. 17-46, 2005.
- [13] W. Lacarbonara, G. Rega, and A. H. Nayfeh, "Resonant non-linear normal modes. Part I: analytical treatment for structural one-dimensional systems," *International Journal of Non-Linear Mechanics*, vol. 38, pp. 851-872, 2003.
- [14] A. H. Nayfeh, *Introduction to perturbation techniques*. New York: Wiley, 1981.
- [15] A. H. Nayfeh and D. T. Mook, *Nonlinear Oscillations*. New York: John Wiley and Sons, 1979.
- [16] M. Peeters, R. Vigu  , G. S  randour, G. Kerschen, and J. C. Golinval, "Nonlinear normal modes, Part II: Toward a practical computation using numerical continuation techniques," *Mechanical Systems and Signal Processing*, vol. 23, pp. 195-216, 2009.
- [17] M. Peeters, G. Kerschen, J. C. Golinval, C. Stephan, and P. Lubrina, "Nonlinear Normal Modes of a Full-Scale Aircraft," presented at the 29th International Modal Analysis Conference (IMAC XXIX), Jacksonville, Florida, 2011.
- [18] R. R. J. Craig, *Structural Dynamics*. New York: John Wiley and Sons, 1981.
- [19] J. J. Hollkamp, R. W. Gordon, and S. M. Spottswood, "Nonlinear modal models for sonic fatigue response prediction: a comparison of methods," *Journal of Sound and Vibration*, vol. 284, pp. 1145-63, 2005.
- [20] M. I. McEwan, J. R. Wright, J. E. Cooper, and A. Y. T. Leung, "A COMBINED MODAL/FINITE ELEMENT ANALYSIS TECHNIQUE FOR THE DYNAMIC RESPONSE OF A NON-LINEAR BEAM TO HARMONIC EXCITATION," *Journal of Sound and Vibration*, vol. 243, pp. 601-624, 2001.
- [21] A. A. Muravyov and S. A. Rizzi, "Determination of nonlinear stiffness with application to random vibration of geometrically nonlinear structures," *Computers & Structures*, vol. 81, pp. 1513-1523, 2003.
- [22] S. A. Rizzi and A. Przekop, "Estimation of Sonic Fatigue by Reduced-Order Finite Element Based Analyses," presented at the IX International Conference on Recent Advances in Structural Dynamics, Southampton, UK, 2006.
- [23] R. W. Gordon, J. J. Hollkamp, and S. M. Spottswood, "Nonlinear response of a clamped-clamped beam to random base excitation," presented at the Eighth International Conference on Recent Advances in Structural Dynamics, University of Southampton, Southampton, UK, 2003.
- [24] R. D. Cook, D. S. Malkus, M. E. Plesha, and R. J. Witt, *Concepts and Applications of Finite Element Analysis*, Fourth ed.: John Wiley and Sons, 2002.